

Heavy Flavor measurements using high- p_T electrons in the ALICE EMCAL

Mark T Heinz (for the ALICE collaboration)

Yale University, WNSL, 272 Whitney Ave, New Haven, CT 06520, USA

E-mail: mark.heinz@yale.edu

Abstract. Heavy flavor hadrons, i.e. those containing charm and bottom quarks, will be abundantly produced at the LHC and are important probes of the Quark-Gluon Plasma (QGP). Of particular interest is the investigation of parton energy loss in the medium. Using heavy flavor jets we will have a pure sample of quark jets with which to study the color-charge effects on energy loss. In addition, studies of bottom production in p+p collision at LHC energies will be utilized to further constrain the current parameters used by NLO and FONLL calculations. The talk will focus on the very high-pt electron particle identification using the EMCAL detector. We present the electron reconstruction and measurements which can be achieved with 1 nominal year of Pb-Pb running at $\sqrt{s}=5.5$ TeV. We then estimate the rate of non-photonic electrons and present systematic and statistical error bars. Finally, we show preliminary results on B-jet tagging techniques in p+p which utilize jet-finding algorithms (FASTJET) in conjunction with displaced secondary vertices containing high-pt electrons.

1. Introduction

From a heavy ion physics point of view the interest is focussed on the parton energy loss for quarks and gluons in the strongly interacting medium produced by the heavy ion collisions. Heavy flavor quarks provide excellent probes since they are produced at early times in the collisions and need to traverse the Quark-Gluon Plasma (QGP). At intermediate p_T , the prediction that the energy loss of massive quarks in a colored medium is reduced due to the suppression of forward radiation (“dead cone effect” [1]) has not been validated by measurements at RHIC [2, 3], which find heavy flavor production at high p_T to be suppressed at the same level as light flavor quarks and gluons. Beyond the energy range where the dead cone effect is expected to be significant (i.e. $E_T \gg m$), heavy quark jet production may provide a tool to probe the color-charge dependence of energy loss [4]. This is illustrated in Fig. 1 where one can see that the modification, quantified by the nuclear modification factor R_Q , between charm and bottom quarks becomes comparable for $p_T > 20$ GeV/c. However the ratio between light quarks and gluons remains constant at $\sim 9/4$ due to the color Casimir factor. In a more speculative vein, modelling of heavy “quark” propagation in a strongly coupled fluid using the techniques of AdS/CFT has received significant recent attention [5], including a suggestion that the relative suppression of charm vs. bottom quarks is different in pQCD and AdS/CFT, with a magnitude that could be resolvable by experiment [6].

In addition, with the first p-p data obtained at 7 TeV basic measurements such as jet cross-sections, jet-profiles and jet fragmentation-functions of heavy flavor jets will allow us to make important tests of NLO and MLLA calculations.

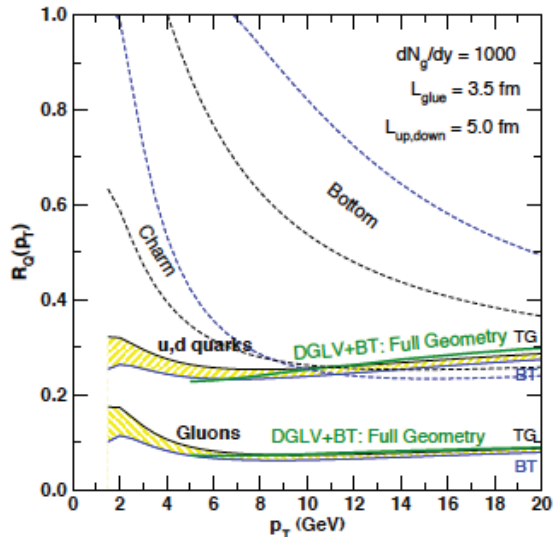


Figure 1. Theory calculations of quark and gluon nuclear modification factors at RHIC from the DGLV model [7]

The ALICE experiment is well suited to perform the measurements of heavy flavor production at high p_T . While exclusive reconstruction of charm mesons will be carried out via the use of the TPC and ITS detectors, measurements of high p_T heavy flavor production require a fast trigger, which is possible only for the semi-leptonic decay mode, with a branching ratio of $\sim 10\%$. The TRD has an efficient electron trigger and good hadron rejection for $p_T < 10$ GeV/c, but at higher p_T additional tools are required for heavy flavor measurements. The EMCAL has excellent capabilities for fast triggering and hadron rejection, and provides unique coverage in ALICE for heavy flavor measurements at very high p_T (above 10 GeV/c), and the following studies are therefore focused on that region.

In addition the EMCAL together with the central tracking system will also allow for full jet reconstruction. Jets are the primary experimental observable for partons. Combining the jet-finding with heavy flavor tagging techniques will allow us to obtain a reasonably clean sample of heavy flavor jets. These tagging techniques were developed by the Fermilab experiments (see for example [8]). We will present the results from the implementation of the displaced secondary vertex method which uses heavy flavor electrons as "seed" particles.

2. High p_T Electron Rates

The goal of this section is to establish the expected p_T reach of heavy flavor hadrons in a Pb-Pb run and determine the dominant background sources. The primary physics sources of electrons at high p_T are the semi-leptonic decays of charm (C) and bottom (B) hadrons (mostly mesons), and the decay of W-bosons. Electrons from C-hadron decay come both from prompt charm production and secondary decay of C-hadrons produced by the hadronic decay of B-hadrons.

In addition, there are significant backgrounds to these sources, due both to other physical processes and detector effects. The physics backgrounds consist primarily of electrons from Dalitz decays of high p_T π^0 and η hadrons in jet fragmentation and to a lesser extent quarkonia decays (not studied here), while the dominant detector source are photon conversions in the ITS and beampipe which are tracked in the TPC.

To obtain the expected annual yields of single electrons in the EMCAL, a sample of PYTHIA

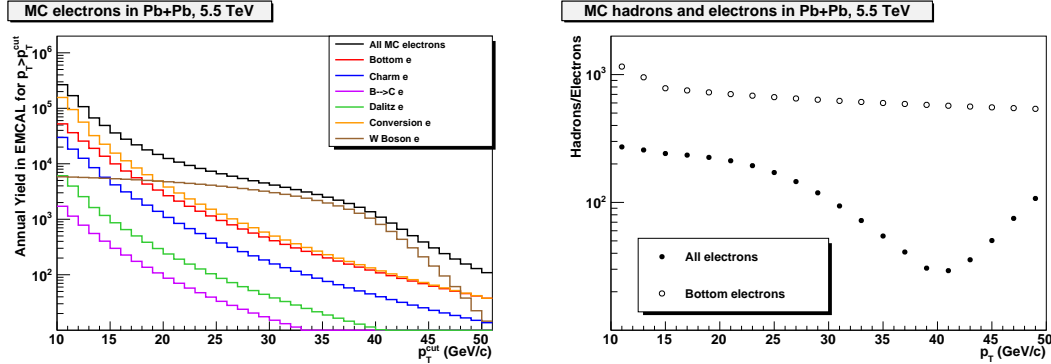


Figure 2. (left) Rates of MC-Electrons from the various physics/detector sources shown as the integrated annual yield above a p_T -cut for a nominal ALICE Pb–Pb year at $\sqrt{s_{NN}} = 5.5 \text{ TeV}$. (right) Ratio of charged hadrons to electrons at the particle level expected in Pb–Pb events. The dip near 40 GeV/c is due to the contribution of W-decay electrons.

p-p collisions at 5.5 TeV, triggered on specific subprocesses, was simulated. A large sample of inclusive jet events, with one jet constrained to point towards the EMCal acceptance, was analyzed to evaluate the dominant physics and detector backgrounds. A smaller sample of W-boson events was generated to estimate the contribution from W-decay. The signal events were created using the ALICE standard PYTHIA heavy-flavor settings and requiring a B-jet in the EMCal acceptance and the B-hadron to decay semi-leptonically.

The left panel of Fig. 2 shows the contributions of the different physics sources to the distribution of electrons in the EMCal acceptance. Yields correspond to the expected Pb–Pb luminosity of $0.5 \text{ mb}^{-1}\text{s}^{-1}$ and one month (10^6 s) of Pb–Pb running to obtain an annual yield.

From this figure it is clear that there is a significant rate of bottom electrons to $p_T \sim 50 \text{ GeV}/c$ in the EMCal. The dominant backgrounds to heavy flavor electrons come from the photon conversions and from W-boson decays for $p_T > 20 \text{ GeV}/c$. The other significant background to measuring B-electrons will be from charged hadrons misidentified as electrons. In order to evaluate the minimum hadron rejection required by the electron identification algorithm, the ratio of charged hadrons to electrons from the same simulation is shown in the right panel of Fig. 2. The ratio for transverse momentum in the range of interest from 10-50 GeV/c is a few hundred, which sets the scale for the hadron rejection requirement.

3. Electron Identification

The method of identifying electrons in the EMCal relies on the fact that electrons deposit all of their energy in the EMCal while hadrons typically leave only a small fraction (i.e. MIP) of their energy in the EMCal. In order to calculate the ratio of EMCal energy to reconstructed track momentum, tracks are matched to EMCal clusters. The procedure takes a reconstructed track and extrapolates it to the EMCal. If the distance between the extrapolated track-position and any cluster-position is less than a given value (in this study about the size of 1 tower) then the track is considered to be matched. In a second loop the matches are compared and only the closest matches are kept, thereby eliminating competing pairs.

We use the matched cluster-track pairs, the cluster energy, and the reconstructed track momentum to calculate the E/p ratio. This distribution is shown in Fig. 3 for single electron and pion tracks for two different momenta. The normalization of the two distributions is arbitrary and does not reflect the respective ratio of pions to electrons. The effect of particle interactions with the detector material is shown for each species. This was done by comparing the MC-input

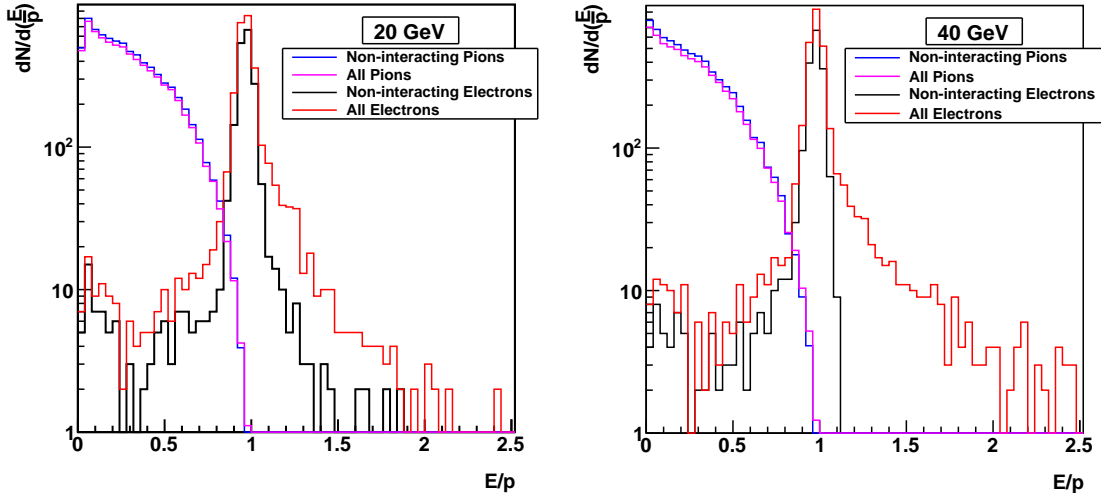


Figure 3. E/p distributions for single electrons and pions at momenta of 20 GeV/c (left) and 40 GeV/c (right). The normalization of the particle species relative to each other is arbitrary. The lines marked “non-interacting” refer to particles that lose less than 10% of their momentum before arriving at the EMCAL surface.

to the reconstructed momentum. If the particle had lost more than 10% of its input momentum it was considered to have interacted with the detector material and labeled “interacting”. If, on the other hand, the reconstructed momentum was more than 90% of the input momentum then it was considered “non-interacting”. Electrons are known to suffer bremsstrahlung in the detector material as can be seen in the slight “tails” of the E/p distribution towards the larger values.

We establish an electron identification criterion by setting a lower limit on the E/p ratio. We define the efficiency, ϵ , as the number of electrons that pass the cut divided by the total number of electrons in our sample. One can then estimate the amount of hadron contamination by integrating the counts above the cut value. This determines the rejection power of the method, defined as ϵ^{-1} for pions. The actual electron purity in a p-p (Pb-Pb) collision will depend on the relative ratio of pions to electrons in the data.

On the left hand side of Fig. 4 the hadron rejection power is plotted as a function of cluster energy and compared to the recently published 2007 CERN-SPS test-beam data [9]. The results between simulation and real data are consistent if one considers non-interacting particles in the simulation.

The right hand side of Fig. 4 shows the results for hadron rejection power using a full GEANT simulation of the ALICE detector material. In simulations with large hadronic and photonic backgrounds (PYTHIA, HIJING) we determined that an additional cut on EMCAL cluster shape and size was necessary to ensure that the electron clusters are correctly identified. This comes at the expense of electron efficiency, which drops to $\sim 65\%$. With these cuts the rejection power still reaches 1000 at 40 GeV/c, yielding a resulting electron/hadron ratio of at least 3:1.

4. Reconstructed Electron Spectra

Utilizing the PID capabilities of the EMCAL we can now reconstruct inclusive and non-photonic electron (NPE) spectra. In order to remove the photonic conversion electrons from the inclusive sample, all candidate electrons are checked against the list of reconstructed secondary vertices

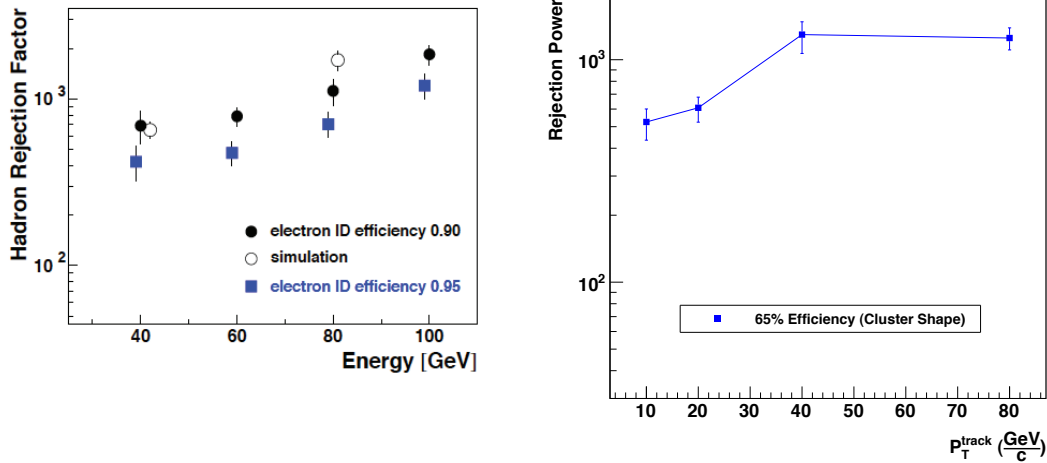


Figure 4. Hadron rejection factor as a function of electron efficiency and energy/momentum. (left) Simulation results compared to 2007 CERN test-beam data [9]. (right) Results from simulation with full detector material and optimized cuts for PYTHIA and HIJING multiplicities using cluster-shape and size criteria. The tracks used are required to have at least 50 TPC hits and 3 ITS hits.

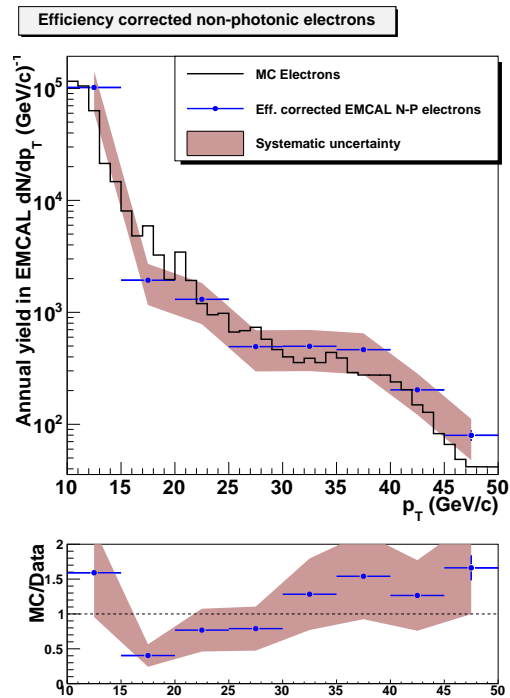


Figure 5. Efficiency corrected signal of non-photonic electrons for EMCAL PID compared to MC truth for bottom and W-decay electrons. Systematic errors due to varying the EMCAL electron identification criteria are shown.

(V0) created from charged particles. Those matching a V0 with invariant mass near that of

a photon, ρ^0 , ω or ϕ hadron are considered “photonic” and are subtracted from the inclusive spectrum to obtain the NPE candidate yield.

To determine the total yield of non-photonic electrons, the estimated contamination from misidentified hadrons is subtracted from the inclusive NPE candidate spectrum and the resulting signal distribution is corrected by the efficiency. The result of these operations is presented in Fig. 5. The efficiency corrected spectrum is in agreement with the MC-input distribution within the systematical uncertainties. The systematic uncertainty bands were determined by varying the track-matching and electron identification cuts in several combinations. The decreased efficiency resulting from tighter cuts is compensated by the increased purity and vice versa. With these simulations we obtain point-by-point uncertainties that vary by less than a few percent about an average value of $\sim 40\%$. Additional systematic effects, in particular in conjunction with the reconstruction of conversion electrons, still need to be evaluated.

5. B-Jet Tagging: Displaced Vertex Method (“DVM”)

This tagging method relies on the reconstruction of displaced secondary vertices from semi-leptonic B-decays, which are typically displaced by a few hundred μm from the primary vertex. It has been used by CDF to identify bottom contributions in semi-leptonic muon decays [10]. In addition, bottom decays typically produce a large number of charged particles by decaying via charm mesons to lighter hadrons. The highest p_T hadrons are correlated in phase-space and all point back to a common, displaced vertex. By identifying the semi-leptonic displaced vertex consistent with the B-meson lifetime and at least one additional hadron from the decay we have a powerful tool to discriminate non-bottom electrons from bottom electrons.

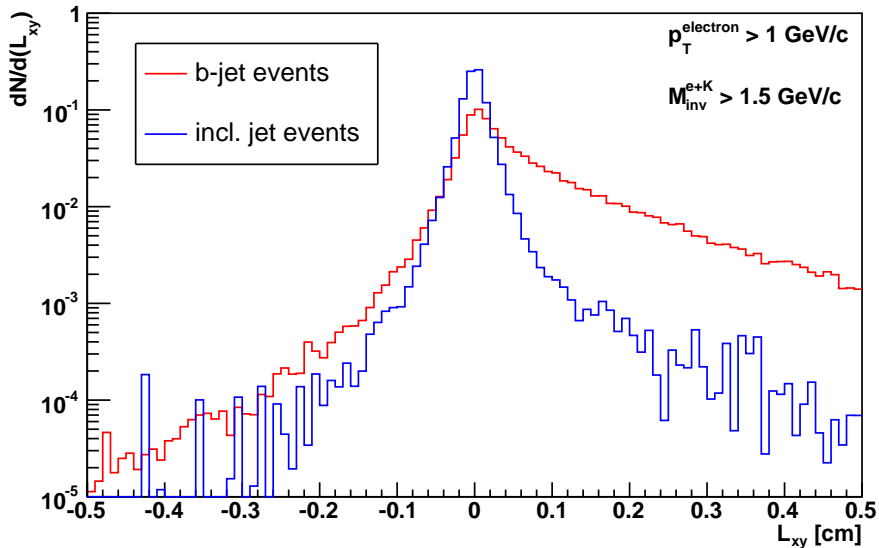


Figure 6. Signed DCA (L_{xy}) distributions from a sample of b-jet events (“Signal”) and inclusive jet events (“Background+Signal”) at 5.5 TeV. The distributions are normalized to the same integral. The inclusive jet events also contain a small contribution of b-jets that was not subtracted.

The method uses a high p_T electron within a jet as a seed, then searches for intermediate p_T hadrons (above 1.0 GeV/c) from a common secondary, displaced vertex within a cone of $R = \sqrt{\Delta\eta^2 + \Delta\phi^2} < 1.0$ around the trigger. This R value was successfully used by CDF but

still needs to be optimized for the heavy ion environment [10]. Electrons below p_T 10 GeV/c are identified using the combined PID of TPC, TRD and EMCAL, whereas above this cut EMCAL PID only is used to guarantee sufficient purity of the sample. A minimum of 4 (out of 6) ITS hits are required on both tracks to ensure sufficient spatial resolution of the secondary vertex. Once a pair is found and its displaced vertex determined, the quantity L_{xy} (in the bending plane) is calculated:

$$L_{xy} = \frac{\mathbf{r} \cdot \mathbf{p}_e}{|\mathbf{p}_e|} = |\mathbf{r}| \cdot \cos(\theta) \quad (1)$$

Where \mathbf{r} is the vector from the primary vertex to the secondary vertex and \mathbf{p} is the electron momentum. The distribution of this quantity is symmetric around zero for the background, but strongly biased towards positive values for real decays. Fig. 6 shows the distributions of L_{xy} for electrons from inclusive jet (“Background+Signal”) and b-jet (“Signal”) events. More details can be found in reference [11].

Based on the distribution of L_{xy} we define cuts to select electrons from b-decays. In this study we have adopted preliminary cuts that require at least n ($n=1,2,3,\dots$) tracks from secondary vertices with $L_{xy} > 0.1\text{cm}$ and $M_{inv}^{e+K} > 1.5\text{ GeV}$. Cutting on the invariant mass is a powerful discriminator to reject semi-leptonic vertices from charm.

The next step consists of identifying such tagged electrons within jets. For this we ran a jetfinder algorithm (FASTJET) on our data and then compared the charged jet constituents to our collection of tagged electrons. If a jet contained a tagged electron it was tagged as a b-jet. All jets first had to pass EMCAL acceptance criteria in η , ϕ and neutral energy fraction to ensure complete reconstruction of the neutral and charged components.

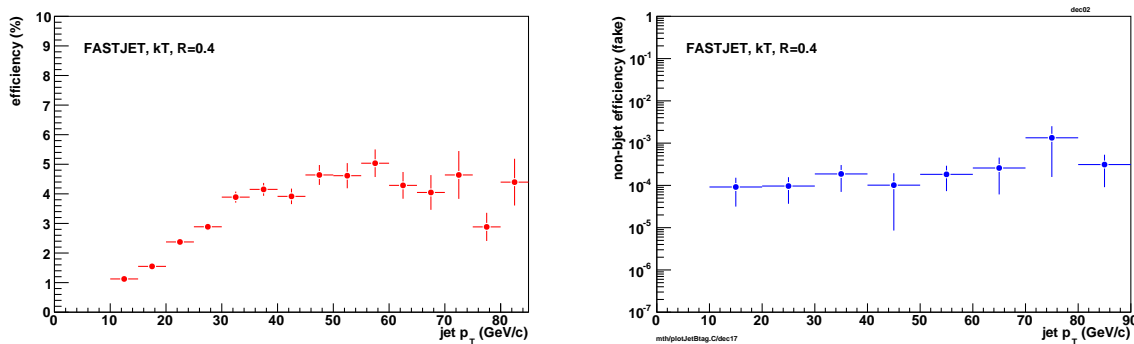


Figure 7. Tagging efficiency (left) and fake rate (right) for DVM B-tagging as a function of reconstructed jet p_T . These results were obtained requiring at least 2 displaced vertices. Jets were reconstructed using the k_T -algorithm of the FASTJET package with $R=0.4$.

In Fig. 7 the current results of the DVM B-tagging algorithm are shown as a function of reconstructed jet p_T . With the algorithm configured for highest purity we currently achieve an efficiency of about 5% for $p_T > 40\text{ GeV/c}$ as compared to MC-input B-jets. This efficiency is expected since we require one high p_T electron and two hadrons from the secondary displaced vertex. The fake tag rate, defined as the efficiency of tagging a non-B jet, is of the order of 10^{-4} which means that the purity of the tagged sample, depending on the input model, is well above 90%. In figure 8 we show the estimated amount of tagged B-jets from one nominal year of Pb-Pb running which confirms that our statistical reach is up to p_T of $\sim 60\text{ GeV/c}$. These studies are still preliminary and work is ongoing to optimize the efficiency versus fake rate of the algorithm.

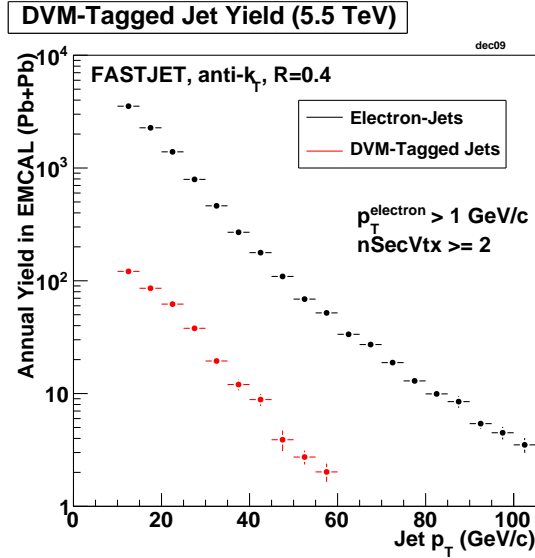


Figure 8. Final yield per Pb-Pb year of B-tagged jets using the FASTJET anti- k_T -algorithm and the DVM tagging method.

6. Conclusions

We have shown that the EMCAL possesses excellent electron PID capabilities and extends ALICE's electron PID in the p_T range up to 80 GeV/c, with hadron rejection factors of the order of several hundreds. This capability will allow to measure non-photonic electrons in Pb-Pb collisions for p_T ranges well above that previously reported at RHIC, and thus gain insight into color-charge and/or quark mass effects of partonic energy loss. Further studies for effectively reducing conversion and W-boson backgrounds are underway. The studies of B-tagging are at a proof-of-principle stage. We have shown that the displaced secondary vertex algorithm yields good results in p-p collisions and allows to measure B-jets up to a jet- p_T of ~ 60 GeV/c. We expect to further optimize the algorithm to find an optimal balance between efficiency and purity.

References

- [1] Y.L. Dokshitzer, and D.E. Kharzeev, *Phys. Lett.* **B519** (2001) 199
- [2] A. Adare et al. (PHENIX coll), *Phys. Rev. Lett.* **98** (2007) 172301
- [3] B.I. Abelev et al. (STAR coll.), *Phys. Rev. Lett.* **98** (2007)192301
- [4] N. Armesto et al., *Phys. Rev.* **D71** (2005) 054027
- [5] S.S. Gubser, arXiv:0907.4808
- [6] W.A. Horowitz and M. Gyulassy, *Phys. Lett.* **B666** (2008) 320
- [7] S. Wicks et al., *Nucl. Phys.* **A784** (2007) 426
- [8] D. Acosta et al. (CDF coll.), *Phys. Rev.* **D69** (2004) 072004
- [9] J. Allen et al. *Nuclear Inst. and Methods in Physics Research A* **615** (2010) 6-13.
- [10] D. Acosta et al. (CDF Coll.), *Phys. Rev.* **D66** (2002) 014003
- [11] M. Heinz for the ALICE collaboration, arXiv:0712.2422